RSC Advances

PAPER

View Article Online
View Journal | View Issue

Cite this: *RSC Adv.*, 2023, **13**, 30539

Using phenolic polymers to control the size and morphology of calcium carbonate microparticles†

Yurie Nakanishi,[a] Bohan Cheng,[a] Joseph J. Richardson[ab] and Hirotaka Ejima *[a]

Calcium carbonate ($CaCO_3$) is a naturally occurring mineral that occurs in biology and is used industrially. Due to its benign nature, $CaCO_3$ microparticles have found use in the food and medical fields, where the specific size of the microparticles determine their functionality and potential applications. We demonstrate that phenolic polymers with different numbers of hydroxy groups can be used to control the diameter of $CaCO_3$ microparticles in a range of 2–9 μm, and obtained particles were relatively uniform. The largest particles (~9 μm in diameter) were obtained using poly(2,3,4,5-tetrahydroxystyrene) (**P4HS**), which showed the highest water solubility among the tested phenolic polymers. The polymer concentration and stirring speed influenced the size of microparticles, where the size of the obtained particles became smaller as the concentrations of phenolic polymers increased and as the stirring speed increased, both likely due to promoting the formation of a large number of individual crystal seeds by shielding seed–seed fusion and increasing the chances for precursor contact, respectively. The preparation time and temperature had a great influence on the morphology of the $CaCO_3$ particles, where vaterite transforms into calcite over time. Specifically, aragonite crystals were observed at preparation temperature of 80 °C and vaterite particles with rough surfaces were obtained at 40 °C. Molecular weight and scale of reaction were also factors which affect the size and morphologies of $CaCO_3$ particles. This research represents a facile method for producing relatively monodisperse $CaCO_3$ microparticles with diameters that have previously proven difficult to access.

Received 17th July 2023
Accepted 9th October 2023

DOI: 10.1039/d3ra04791a

rsc.li/rsc-advances

Introduction

Calcium carbonate ($CaCO_3$) is one of the most abundant inorganic minerals naturally found in the exoskeletons of algae, eggshells, mussel shells, and sea urchin spines.[1] It is also an important compound actively used in biomedical and industrial applications, such as drug delivery, paper manufacturing, cosmetics, fillers, and rubber.[2] $CaCO_3$ has six different polymorphs:[3] amorphous calcium carbonate (ACC), calcium carbonate hexahydrate, calcium carbonate monohydrate, vaterite, aragonite, and calcite. Among these six polymorphs, ACC is the least stable phase and transforms into one of the crystalline polymorphs unless stabilized with specific additives.[4,5] Of the crystalline phases, calcite is the most stable at room temperature and pressure, and vaterite is the least stable that rarely occurs in nature.[6] Recently, the controlled synthesis and crystallization of $CaCO_3$ have been investigated because controlling the size and morphology of $CaCO_3$ particles is of particular importance for applications such as drug delivery.[7]

The simplest synthesis method of $CaCO_3$ spheres is *via* the vigorous mixing of solutions of $CaCl_2$ and Na_2CO_3,[8] where formation and crystallization generally follow Ostwald's rules of states.[3,9] After mixing, $CaCO_3$ temporarily exists as amorphous calcium carbonate (ACC), which rapidly transforms into more stable crystals. As this precipitation process is very rapid, a mixture of polymorphs and polydisperse particles form, and therefore controlling the size and morphology of these $CaCO_3$ particles are generally challenging. To control the crystal growth and particle size of $CaCO_3$, certain stabilizing polymers can be added to the precipitation solution to control precipitation in two main ways.[10] First, the hydroxy, carboxy, or sulfonic groups on the polymer chains can complex with Ca^{2+} in the mixed solution due to electrostatic interactions, thereby delaying nucleation. This allows for the nano-sized amorphous intermediates to aggregate and gradually crystallize. The second effect of the polymer is to bind to the surface of these aggregated amorphous intermediates and prevent particles from growing along a particular crystal plane. As a result, the particles aggregate spherically and grow into microscale spherical particles, where recrystallization into more stable structures is inhibited.

Many anionic polymer additives such as polystyrene sulfonate (PSS),[11–16] poly(acrylic acid) (PAA),[4,17–22] poly(vinylsulfonic acid) (PVSA),[23] and double hydrophilic block copolymers

[a]*Department of Materials Engineering, The University of Tokyo, 7-3-1 Hongo, Bunkyo-ku, Tokyo 113-8656, Japan. E-mail: ejima@g.ecc.u-tokyo.ac.jp*
[b]*School of Engineering, RMIT University, Melbourne, VIC 3000, Australia*

† Electronic supplementary information (ESI) available. See DOI: https://doi.org/10.1039/d3ra04791a

(DHBC)[24–27] have shown a profound effect on crystallization. Furthermore, precipitation conditions such as pH,[3,25] temperature,[28,29] polymer concentration,[2,30] incubation time,[31,32] and stirring speed[33] impact the size, dispersity, and polymorphs of $CaCO_3$. Despite the numerous efforts devoted to the controlled synthesis of $CaCO_3$ particles, a systematic study of monodisperse particles bigger than 4.0 μm has yet to be achieved and remains challenging. The possible reason for the difficulty in preparing particles with a large particle size is that it is difficult to achieve both delaying nucleation and effectively stimulating nucleation growth at the same time. For example, one effective way to delay nucleation is increasing the concentrations of polymers. Higher polymer concentration means providing the more chelation sites for Ca^{2+}. However, those higher amounts of polymer would prevent particles from growing or provide more nucleation sites, and it results in the particles with a small diameter. We could obtain bigger particles by decreasing the polymer concentration because a lower amount of polymer doesn't prevent particles from growing, but the resulting particles become very heterogeneous. This is because the Ca^{2+} is not chelated well, so the nucleation is not delayed, and it results in the uncontrolled heterogeneous nucleation growth. Most of the studies that have already been reported to obtain large fine particles by polymer addition method are not uniform in particle size or contain various crystal polymorphs. Based on these results, new polymers that can simultaneously delay nucleation and promote nucleation growth are required to obtain bigger and uniform $CaCO_3$ particles.

We recently reported the synthesis of phenolic polymers with three, four, and five hydroxy groups on one styrene monomer unit, and demonstrated their ultrastrong underwater adhesion.[34,35] The number of hydroxy groups determined the underwater adhesion strength and it is known that catechol (2 hydroxy groups) and gallol (3 hydroxy groups) have an affinity for metal ions. We hypothesized that the number of hydroxy groups of phenolic polymers could also play an important role in the chelation of Ca^{2+} ions, and therefore might be able to control the crystallization of $CaCO_3$. Herein, five kinds of phenolic polymers, poly(4-hydroxystyrene) (**P1HS**), poly(3,4-dihydroxystyrene) (**P2HS**), poly(3,4,5-trihydroxystyrene) (**P3HS**), poly(2,3,4,5-tetrahydroxystyrene) (**P4HS**), and poly(2,3,4,5,6-pentahydroxystyrene) (**P5HS**) were used as polymer additives for $CaCO_3$ crystallization (Fig. 1a), and $CaCO_3$ particles with diameters ranging from 2 to 9 μm were successfully synthesized. The largest particles were obtained when using poly(2,3,4,5-tetrahydroxystyrene) (**P4HS**), which showed the highest water solubility among the tested phenolic polymers. Moreover, the stirring speed, concentration of phenolic polymers, molecular weight of phenolic polymers, and the scale of reaction also influenced the crystal size, while the temperature and preparation time influenced the morphology. Based on these experimental results, the mechanism of $CaCO_3$ crystallization in the presence of phenolic polymers was discussed. The current research presents a facile method to produce relatively uniform $CaCO_3$ microparticles and has a potential in applications that require larger microparticles, such as porous scaffold materials[36] or orally administered drug delivery vehicles.[37]

Experimental details

Chemicals and materials

The syntheses of phenolic polymers were carried out as reported by Cheng *et al.*[34] Calcium chloride ($CaCl_2$), sodium carbonate (Na_2CO_3) and methanol were purchased from FUJIFILM Wako Pure Chemical, and used without further purification.

Preparation of $CaCO_3$ particles

We prepared $CaCO_3$ particles using a simple mixing method of two solutions. Typically, 240 μL of 1 M $CaCl_2$ solution was added to 19 mL of 12 mM Na_2CO_3 ($[Ca^{2+}] \sim 24$ mM, $[CO_3{}^{2-}] \sim 12$ mM) solution containing phenolic polymers (**P1HS**–**P5HS**) at room temperature. As for **P1HS**–**P3HS**, equal volumes of polymer/methanol solution prepared at 10 mg mL^{-1} were added, and then pure water was added to the solution because the water solubilities of these phenolic polymers are lower than **P4HS** and **P5HS**. Although the solvent plays a key role in controlling the growth, polymorphism, and the shape of $CaCO_3$ particles,[38,39] the methanol added in our experiment accounted for only 1 vol% of the total solvent, and therefore the solubility of **P1HS**, **P2HS**, and **P3HS** in the mixed solutions was still low. The addition of methanol had a negligible effect on the size of $CaCO_3$ particles. The polymer concentration was varied in the range of 0–0.5 mg mL^{-1} and the reaction temperature was varied in the range of 25–80 °C. After mixing, the solution was stirred for 60 s. Stirring speed differs in the range of 500–1500 rpm. The precipitated $CaCO_3$ was soon collected by centrifugation (5000*g*, 60 s) and washed twice with DI water. Typically, the precipitates were collected soon after the stirring, but the precipitates were kept without any treatment for 0 min to 7 days in order to examine the effect of preparation time. After centrifugation, the resulting particles were calcined at 500 °C for 2 h to remove the remaining phenolic polymers.

Characterization

The number-average molecular weight (M_n) and polydispersity index (PDI) of phenolic polymers were both measured by gel permeation chromatography (Prominence-i GPC System, SHIMADZU, Japan) using THF as the eluent. The calibration curve was prepared using polystyrene standards. Water solubilities of phenolic polymers were measured by dissolving excess polymer in 10 mL DI water at room temperature. The mixture was sonicated for 30 min and aqueous solutions of the polymers were filtered. The filtrate was collected and weighed after freeze-drying using a FDS-2000 freeze-drier (EYELA, Tokyo, Japan). Water solubility was then calculated by the weight of polymer remaining. The size of the $CaCO_3$ particles was measured using an inverted optical microscope (Eclipse TE2000, Nikon, Japan). $CaCO_3$ particles were observed under the microscope with a 40× objective lens immediately after centrifugation. 100 particles were analysed for each sample to calculate mean values and standard deviations. A coefficient of variation (CV) was calculated by dividing standard deviation by the mean value. The calcined $CaCO_3$ samples were dispersed in DI water and dropped on silicon substrates. They were dried at room temperature,

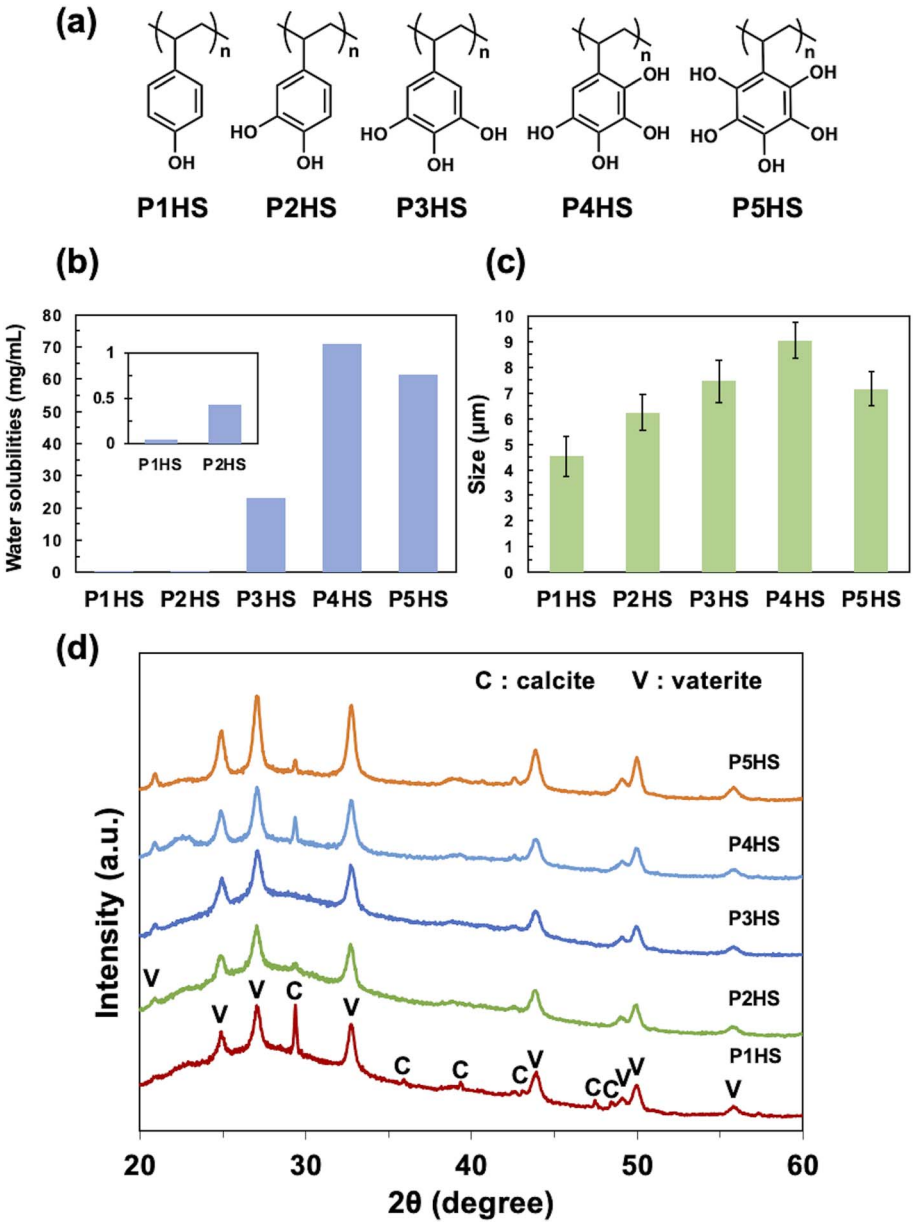

Fig. 1 (a) Chemical structures of poly(4-hydroxystyrene) (**P1HS**), poly(3,4-dihydroxystyrene) (**P2HS**), poly(3,4,5-trihydroxystyrene) (**P3HS**), poly(2,3,4,5-tetrahydroxystyrene) (**P4HS**), and poly(2,3,4,5,6-pentahydroxystyrene) (**P5HS**). (b) Water solubilities of the different phenolic polymers. (c) The average size of $CaCO_3$ particles obtained in the presence of the phenolic polymers (0.1 mg mL^{-1}). (d) XRD patterns of $CaCO_3$ particles obtained in the presence of the phenolic polymers (0.1 mg mL^{-1}).

then platinum was sputtered on the surface by a sputter coater (JEC-3000FC, JEOL, Japan). The samples were characterized using a scanning electron microscope (JCM-7000, JEOL, Japan) and a field-emission scanning electron microscope (JSM-7000F, JEOL, Japan) at an accelerating voltage of 5 kV. X-ray diffraction (XRD) patterns were recorded on a Rigaku Mini Flex 600/PTN with Cu-Kα radiation at tube parameters of 40 kV and 15 mA over a scanning range of 2θ from 20° to 60° and a step size of 0.02°. The analysis was conducted soon after the centrifugation in a typical experiment. The polymorphic ratio of calcite and vaterite in the $CaCO_3$ particles was calculated with Rao's equation.[40]

$$f_v = \frac{I_{110v} + I_{112v} + I_{114v}}{I_{110v} + I_{112v} + I_{114v} + I_{104c}}$$

The surface area of the $CaCO_3$ particles was determined using the BET method with nitrogen adsorption and desorption (MicrotacBEL Corp., Japan). To perform microgravimetric measurements, a quartz crystal microbalance (QCM-992A, SEIKO EG&G) was used. The QCM Au chips (9 MHz, Seiko EG&G) were employed as working electrodes. Specifically, 3 μL of a suspension of $CaCO_3$ particles with a certain particle concentration was dropped on the QCM chips and dried for

20 min in an oven at 65 °C before measurement of the frequency change. Thermogravimetric analysis (TGA) curves of the samples were collected using a DTG-60H (Shimadzu, Japan) within a temperature range of 25–800 °C and with the temperature increase rate set as 10 °C min^{-1}.

Results and discussion

Synthesis and water solubility of phenolic polymers

Phenolic polymers (Fig. 1a) were synthesized according to our previous report,[34] and the molecular weights of the synthesized polymers are summarized in Table S1.† The total number of hydroxy groups on a single aromatic ring greatly influenced the water solubility of the polymers (Fig. 1b), where generally increasing the number of hydroxy groups improve the solubilities of polymers (**P1HS** < **P2HS** < **P3HS** < **P4HS**). Although **P5HS** had the highest numbers of hydroxy groups, **P4HS** showed the highest solubility (71 mg mL^{-1}), possibly due to both the high symmetry of **P5HS** and the intramolecular hydrogen bonds hindering interactions with water molecules.

The effect of phenolic polymers on the crystallization of $CaCO_3$

Without any polymer additive, rhombic crystalline $CaCO_3$ particles with a diameter of 2.0–5.0 μm formed (Fig. S1a†) that were a mixture of calcite and vaterite (Fig. S1b†). The addition of **P1HS**, **P2HS**, **P3HS**, **P4HS**, or **P5HS** yielded spherical $CaCO_3$ particles with diameters of 4.53 ± 0.79 μm, 6.24 ± 0.70 μm, 7.45 ± 0.81 μm, 9.04 ± 0.71 μm, and 7.16 ± 0.65 μm (mean ± S.D.), respectively (Fig. 1c). The optical microscope image of $CaCO_3$ particles synthesized in the presence of **P4HS** was shown in Fig. S2.† It is likely that the coordination of the hydroxy groups of the polymers to Ca^{2+} delayed crystallization and shielded the seeds from growing along crystal planes, and therefore produced spherical crystal polymorphs. The coefficients of variation (CV) were about 10% for **P2HS**–**P5HS** and about 17% for **P1HS**. These results suggested that relatively monodisperse $CaCO_3$ particles were obtained. The corresponding XRD results showed both vaterite and calcite peaks although the calcite peak is much lower than that of vaterite (Fig. 1d), as the relative mass percentage of vaterite is over 85% regardless of the type of added polymer. Overall, these results indicated that phenolic polymers have a significant effect on the morphology of $CaCO_3$, even at concentrations as low as 0.1 mg mL^{-1}.

Among the phenolic polymers tested, the largest $CaCO_3$ particles were obtained when using **P4HS**, which has more hydroxy groups per monomer than **P1HS**–**P3HS**. We note that higher numbers of hydroxy groups promoted aggregation of the nanoscale particles that make up $CaCO_3$ particles, because **P4HS** has more chelation sites for Ca^{2+}, which therefore resulted in larger particles. On the other hand, the average particle size in the presence of **P5HS** was smaller than that of **P4HS**, although **P5HS** has one more hydroxy group than **P4HS**. Trushina *et al.*[3] reported that when the viscosity of the precipitation solution is high, the restricted diffusion of Ca^{2+} promotes nucleation and the resulting $CaCO_3$ particles become smaller. The **P5HS** used in this experiment has a larger molecular weight than **P1HS**–**P4HS** (Table S1†) due to limitations in controlling the molecular weight of such a hydroxylated polymer. This is assumed to be a possible reason for the high viscosity of the **P5HS** solution and the inhibition of crystal growth. The solubilities of the polymers correlate with the particle size (Fig. 1b and c), suggesting that the strength of nanoparticle aggregation depends on the solubility of the capping polymers, which in turn can relate to interact with dissolved species, like metal ions, and water molecules.

BET analysis of the $CaCO_3$ particles precipitated in the presence of **P4HS** revealed a surface area of 8.6 m^2 g^{-1}, which is consistent with previously reported values for $CaCO_3$ particles (6.18 and 8.8 m^2 g^{-1}).[41,42] Furthermore, the average pore size was determined to be 37 nm. Those nano-sized pores were all throughout the particles (Fig. S3†). The apparent density of the $CaCO_3$ particles was estimated as 1.4 g cm^{-3} by QCM according to the previously reported method.[41] Considering the density of vaterite (2.7 g cm^{-3}),[43] ~48% of the total volume of the particle is void (*i.e.*, empty). After calcination at 500 °C for 2 h, the density of the $CaCO_3$ particles decreased to 1.2 g cm^{-3} as the remaining **P4HS** was removed and therefore, the void volume increased to ~56%.

The effect of polymer concentrations on the crystallization of $CaCO_3$

To further examine the effects of phenolic polymers on the controlled crystallization of $CaCO_3$ particles, a series of experiments with various polymer concentrations (0.3 mg mL^{-1} and 0.5 mg mL^{-1}, compared with the standard of 0.1 mg mL^{-1}) were carried out. Overall, particles with average diameters ranging from 2.0 to 9.0 μm were obtained at the stirring speed of 500 rpm with varying concentrations (Fig. 2a). The average particle size decreased with increasing concentration for all phenolic polymers tested (Fig. 2b, S4, and S5†), likely due to the higher number of nucleation sites at higher concentrations and the increased polymer shielding hindering fusion and growth along crystal planes. Moreover, the higher the polymer concentration, the more hydroxy groups are available to bind to Ca^{2+}, which results in the formation of more seeds of $CaCO_3$ nanoparticles. As a result, the crystal growth was inhibited and $CaCO_3$ particles with smaller diameters were obtained at higher concentrations, which is consistent with previous studies.[3] The CV values of obtained particles were about 20% or less, which showed that polymer concentrations didn't affect the particle uniformity so much.

Only vaterite peaks were present in the XRD patterns of the $CaCO_3$ particles when the concentration of **P5HS** was 0.5 mg mL^{-1} (Fig. 2c). However, when decreasing the concentration to 0.3 mg mL^{-1}, calcite peaks appeared along with the vaterite peaks, and even larger calcite peaks appeared at 0.1 mg mL^{-1}. Their relative mass percentage of vaterite is 100% (0.5 mg mL^{-1}), 99% (0.3 mg mL^{-1}), and 94% (0.1 mg mL^{-1}), respectively. $CaCO_3$ particles prepared in the presence of **P3HS** showed only vaterite peaks at all the concentrations, however **P1HS**, **P2HS**, and **P4HS** showed both calcite and vaterite peaks

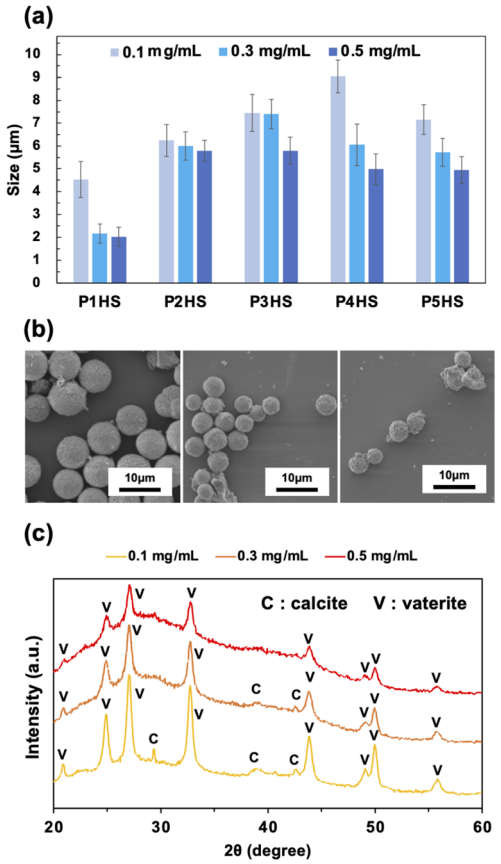

Fig. 2 (a) The relationship between the concentration of phenolic polymers and the final particle sizes. The data for 0.1 mg mL^{-1} are the same as Fig. 1c but also shown here for comparison. (b) SEM images of $CaCO_3$ particles in the presence of **P4HS**. (c) XRD patterns of $CaCO_3$ particles obtained in the presence of **P5HS** with different concentrations.

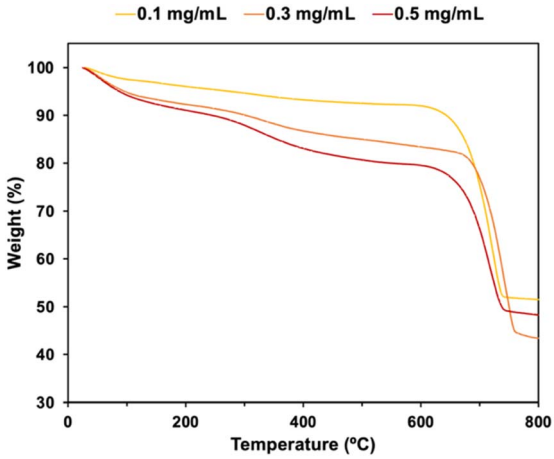

Fig. 3 TGA curves of the $CaCO_3$ particles prepared with **P4HS** at various concentrations.

at 0.1 mg mL^{-1}, but the calcite peaks became smaller as the concentration increased (Fig. S6†). These differences occurred because a large amount of polymer was bound around the $CaCO_3$ particles, which prevented the crystal polymorphs from changing.

The compositions of $CaCO_3$ particles in the presence of **P4HS** were estimated by TGA (Fig. 3). The weight loss between 200 °C and 650 °C were due to the decomposition of the phenolic polymers. At higher polymer concentrations, more polymer molecules were adsorbed on or occluded in the $CaCO_3$ particles, meaning higher polymer concentrations showed a stronger effect on the size of the $CaCO_3$ particles. Distinct thermal decomposition of the polymer and $CaCO_3$ were clearly observed in the TGA curves of the $CaCO_3$ particles prepared with **P1HS** (Fig. S7†). On the other hand, gradual weight losses were observed for **P2HS–P5HS**. This is because PS and **P1HS** decomposed at 400 °C while **P2HS**, **P3HS**, **P4HS** and **P5HS** were partially carbonized and remained in the $CaCO_3$ particles (Fig. S8a†). A sharp peak of graphite (002) in XRD (Fig. S8b†) confirmed that the **P4HS** was partially graphitized during the carbonization process.

Diamond-shaped crystals as well as spherical particles could be observed by scanning electron microscopy (SEM, Fig. S4†), likely because the spherical particles recrystallized into rhombic crystals after precipitation. The obtained $CaCO_3$ particles were aggregates of nanoscale particles as previously reported (Fig. S9a†). The hexagonal-shaped crystals made using 0.5 mg mL^{-1} of **P2HS** indicated that the oriented growth of the microspheres occurred along crystal planes (Fig. S9b†), which is consistent with the fact that $CaCO_3$ particles have a hierarchical architecture composed of oriented nanometric crystals.[11] After calcination at 500 °C, the surface of $CaCO_3$ particles became porous because the phenolic polymers were partially removed (Fig. S9c and d†).

The effect of stirring speed on the crystallization of $CaCO_3$

$CaCO_3$ particles with average diameters ranging from 1.8 to 9.0 μm were obtained at different stirring speeds (1000 rpm and 1500 rpm, compared with the standard of 500 rpm) when using 0.1 mg mL^{-1} of phenolic polymers (Fig. 4). For all polymers, the average size of the $CaCO_3$ particles became smaller as the stirring speed increased, because the coordination of the phenolic hydroxy groups to Ca^{2+} was inhibited when the stirring speed increased and there was higher contact between the precursors, resulting in a higher number of individual seeds, which collectively prevented the formation of larger particles. In the presence of **P4HS**, the average $CaCO_3$ particle size was 9.04 ± 0.71 μm, 4.42 ± 0.65 μm, and 3.56 ± 0.71 μm at stirring speeds of 500 rpm, 1000 rpm, and 1500 rpm, respectively. At 1000 rpm and 1500 rpm, the particle size became smaller, and more rhombic crystals formed, as the interaction between the hydroxy groups of the phenolic polymers and Ca^{2+} was inhibited and mixing was promoted, which resulted in the formation of more stable crystals. The particle size distribution was narrow and did not significantly depend on the stirring speed or type of phenolic polymer added, as relatively uniform $CaCO_3$ particles could be prepared at any stirring speed (Fig. S10 and S11†). The CV values were about 15% or less for **P2HS–P5HS**, and about

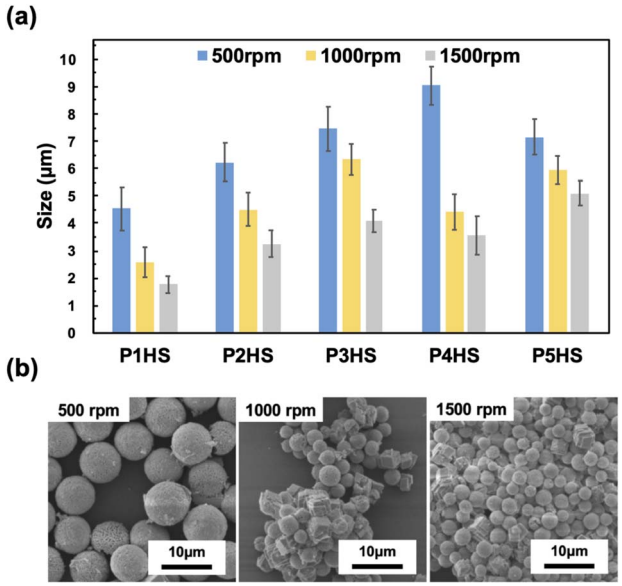

Fig. 4 (a) The relationship between the stirring speed of phenolic polymers and the particle size. The data for 500 rpm are the same as Fig. 1c but also shown here for comparison. (b) SEM images of $CaCO_3$ particles in the presence of P4HS (0.1 mg mL^{-1}) at different stirring speed.

20% or less for **P1HS**. These CV values also confirm that the particle size distribution is narrow.

The effect of temperature on the crystallization of $CaCO_3$

To examine the effect of temperature on the size and morphology of the $CaCO_3$ particles, **P4HS** was used to synthesize $CaCO_3$ particles at different temperatures (40 °C and 80 °C, compared with room temperature). As shown in Fig. 5, significant differences were observed in the morphology of the $CaCO_3$ particles prepared at different temperatures. At 40 °C, particles with rough surfaces were observed (Fig. 5a) and the corresponding XRD peaks (Fig. 5b) were mainly from vaterite. Meanwhile, at 80 °C, needle-like crystals (~6.8 μm) were observed (Fig. 5a) and XRD patterns demonstrated that only aragonite peaks were present (Fig. 5b). This temperature dependence is consistent with previous reports, which discuss the kinetics of formation deeply.[17,44] It is suggested that higher temperature is the favourable condition for the nucleation of aragonite crystals. SEM and XRD of $CaCO_3$ particles prepared at 80 °C in the absence of phenolic polymers (Fig. S12†) demonstrated peaks of vaterite, aragonite, and calcite and a mixture of needle-like crystals and flower-like crystals with diameters much smaller than those prepared with **P4HS** (Fig. 5a). These results indicate that **P4HS** contributed to the growth and stability of needle-like aragonite crystals at 80 °C.

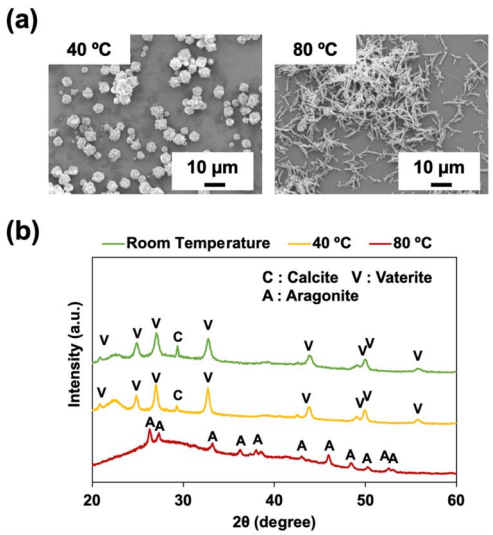

Fig. 5 (a) SEM images of $CaCO_3$ particles in the presence of P4HS (0.1 mg mL^{-1}) at different temperatures. (b) XRD patterns of $CaCO_3$ particles obtained in the presence of P4HS (0.1 mg mL^{-1}) at different temperatures. The data for room temperature are the same as Fig. 1d but also shown here for comparison.

The effect of preparation time on the crystallization of $CaCO_3$

The morphology of the $CaCO_3$ particles prepared with **P4HS** changed depending on the incubation time after stirring for 1 min, where 1 h, 6 h, 12 h, 1 d, 3 d, and 7 d were studied (Fig. 6). As shown in Fig. 6a, the transformation from vaterite to calcite occurred as the preparation time increased, and the calcite crystals became bigger and more complex over time, because the crystal growth proceeded in different directions. The XRD patterns in Fig. 6b clearly show that the calcite peaks became higher and the vaterite peaks became lower over time. The corresponding mass percentage of vaterite was 75% for 1 h, 57% for 12 h, 11% for 24 h, and 0% for 72 h. Taken together, this suggests that $CaCO_3$ particles obtained using **P4HS** as an additive are not stable unless thermal treatment is applied after stirring. However, if the $CaCO_3$ particles were once calcined at 500 °C soon after precipitation, the recrystallization was prevented, and spherical particles were obtained as shown in Fig. 2b. These calcined particles were stable in terms of morphology in DI water for more than 2 months after redispersion. Moreover, XRD patterns of the calcined particles showed that the spherical particles were all calcite (Fig. S13†), confirming that the transformation from vaterite to calcite took place without changing the spherical morphology.

The effect of molecular weight and scale of reaction on the crystallization of $CaCO_3$

To examine the effect of the molecular weight and scale of reaction, **P4HS** was used to synthesize $CaCO_3$ particles at a different molecular weight (M_n ~ 12 kDa, compared with the standard of ~7 kDa) and at different scales of reaction (0.5× scale, and 5× scale, compared with the standard of 1× scale). When $CaCO_3$ particles were prepared with **P4HS** (M_n ~ 12 kDa), particles with diameters of 4.47 ± 0.43 μm were obtained as shown in Fig. S14a.† Compared with those prepared with **P4HS** (M_n ~ 7 kDa), precipitated particles became smaller. As already discussed, the viscosity has an important effect on the size of $CaCO_3$ particles. **P4HS** solution with higher molecular weight

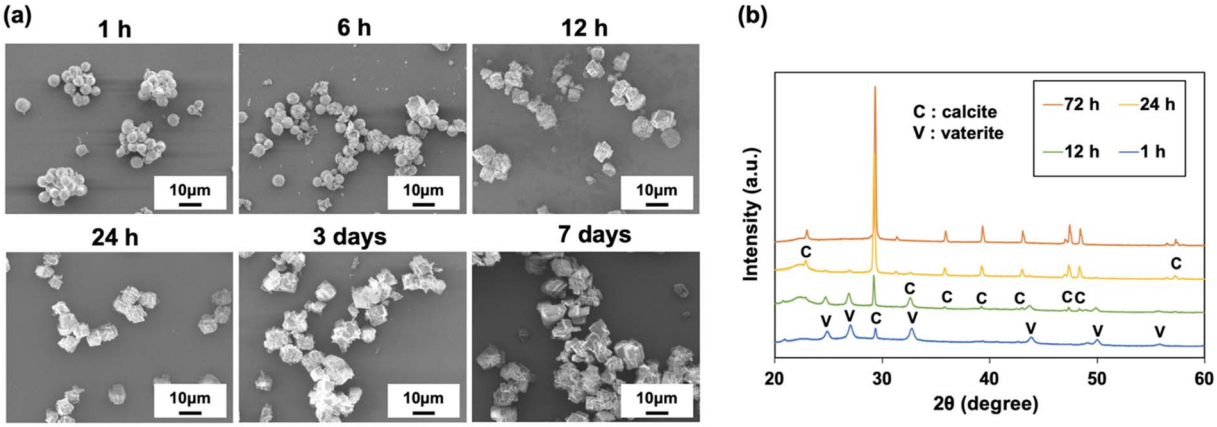

Fig. 6 (a) SEM images and (b) XRD patterns of $CaCO_3$ particles obtained in the presence of **P4HS** (0.1 mg mL^{-1}) at different preparation times.

has a higher viscosity. The inhibition of crystal growth occurred, and the particles became smaller. The corresponding XRD peaks (Fig. S14b†) demonstrated that the crystals obtained were mainly vaterite demonstrating that the length of polymer chain has a negligible effect on the polymorphs of $CaCO_3$ crystals. The effect of scale of reaction was examined by varying the amount of solution added without changing the final concentrations for each of the solutions. The total amount of solution was 20 mL for 1×, and 10 mL for 0.5× scale, and 100 mL for 5× scale. When $CaCO_3$ particles were obtained at 0.5× scale, smaller particles with a diameter of 2.57 ± 0.49 μm were precipitated (Fig. S15a†). The corresponding XRD results (Fig. S15b†) showed both vaterite and calcite peaks. Smaller vaterite particles were obtained because mixing was promoted at smaller scale of reaction, which resulted in the formation of more seeds of $CaCO_3$ nanoparticles. On the other hand, when $CaCO_3$ particles were obtained at 5× scale, heterogeneous particles with a diameter of 5.29 ± 0.69 μm were precipitated (Fig. S15a†). Rough surfaces were observed demonstrating that microparticle were composed of the aggregation of relatively larger grown nanoparticles. At the larger scale of reaction, weaker sheer forces were created, and the growth of nanoparticles was promoted before aggregation. The corresponding XRD results (Fig. S15b†) showed vaterite peaks mainly. From these results, it is suggested that both the molecular weight and scale of reaction had effects on the size of $CaCO_3$ particles.

Discussion

Overall, the effects of six experimental variables were investigated, where polymer concentration, stirring speed, molecular weight, and scale of reaction significantly influenced the particle size, and temperature and incubation time affected the crystal structure and morphology. Specifically, the effect of stirring speed is more prominent than polymer concentration in terms of final particle size. Increasing the concentration of phenolic polymers did not always lead to an increase in the number of nucleation sites because of the low solubilities of **P1HS–P3HS**. Regarding crystal structure and morphology, the effects of both temperature and preparation time are

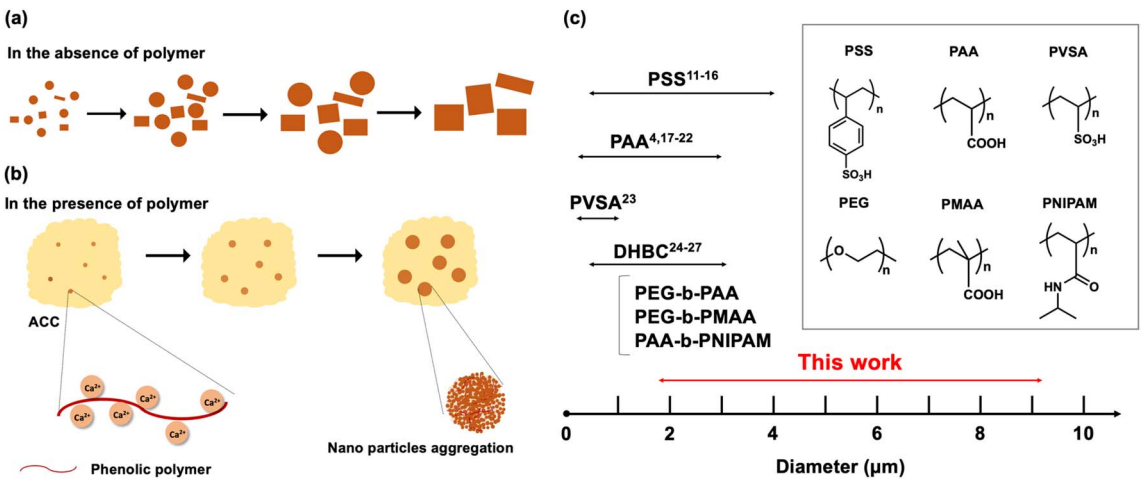

Fig. 7 Proposed mechanisms of $CaCO_3$ growth in the absence (a) and presence (b) of phenolic polymers. (c) The size range of $CaCO_3$ particles obtained in the previous reports compared to the range obtained in this work.

prominent. Three kinds of crystal structures were all observed by changing the reaction conditions. As shown in Fig. S1,† in the absence of polymer, a mixture of calcite and vaterite was found soon after, however, as time goes on the dissolution of vaterite and growth of calcite proceeds in water (Fig. 7a). In the presence of phenolic polymers, the hydroxy groups of the polymers bind to Ca^{2+} and slow the nucleation growth and shield seed fusion. Nano-sized amorphous particles form in solution, and then the amorphous precursors transform into nanosized crystals slowly. Finally, the nanoparticles aggregate and grow into microparticles (Fig. 7b). When increasing the polymer concentration, the number of nucleation sites increased, shielding increased, and the obtained microparticles were relatively small. When the stirring speed was higher, sheer forces were created that drastically increased the number of crystallization nuclei and therefore the obtained microparticles became smaller. The sizes and standard deviations of $CaCO_3$ particles prepared under various conditions using different polymers were summarized in Table S2.† Collectively, the size range of $CaCO_3$ particles obtained in this work was compared to previous reports in Fig. 7c, which highlights the usefulness of phenolic polymers as an additive for $CaCO_3$ particle synthesis.

Conclusions

In summary, $CaCO_3$ particles with relatively uniform particle diameters in the range of 2–9 μm were successfully synthesized by adding polymers with anywhere from one to five phenolic hydroxy groups, and by changing the polymer concentration, stirring speed, temperature, preparation time, molecular weight, and/or the scale of reaction. In particular, the largest monodisperse particles were precipitated in the presence of **P4HS**. The particle diameters of the obtained particles became smaller as the polymer concentration increased, and the particle diameters became smaller when the stirring speed was high. Analysis of XRD patterns showed mainly vaterite peaks at higher polymer concentrations though calcite peaks were also detected at low concentration. Temperature and preparation time affect the morphologies of the obtained crystals. At high temperature (80 °C), needle-like aragonite crystals were easily obtained. When incubated in water, spherical vaterite particles transformed to calcite over time if the particles were not calcined. However, once calcined at 500 °C, the particles kept the initial spherical shape in DI water for at least 2 months. Molecular weight and scale of reaction also affected the size of $CaCO_3$ particles showing that the size of $CaCO_3$ particles is determined by various factors. Our findings introduce a new strategy for producing relatively uniform $CaCO_3$ microparticles with diameters that have previously proven difficult to access.

Author contributions

The manuscript was written through contributions of all authors. All authors have given approval to the final version of the manuscript.

Conflicts of interest

There are no conflicts of interest to declare.

Acknowledgements

This research was partially supported by Japan Society for the Promotion of Science (JSPS) KAKENHI (Grant No. 20H02581 and 20K20641), Japan Science and Technology Agency (JST) through the Precursory Research for Embryonic Science and Technology (PRESTO) grant number JPMJPR21N4 (H. E.) and "Advanced Research Infrastructure for Materials and Nanotechnology in Japan (ARIM)" of the Ministry of Education, Culture, Sports, Science and Technology (MEXT), Grant Number JPMXP1223UT0277. H. E. acknowledges Katsu Research Encouragement Award of the University of Tokyo. J. J. R. acknowledges JSPS for the postdoctoral fellowship for research in Japan (P20373). J. J. R. is the recipient of an Australian Research Council Future Fellowship (project number FT210100669) funded by the Australian Government. Biorender was used for graphical illustrations.

References

1 S. Kim and C. B. Park, *Langmuir*, 2010, **26**, 14730–14736.
2 X. Yang, G. Xu, Y. Chen, F. Wang, H. Mao, W. Sui, Y. Bai and H. Gong, *J. Cryst. Growth*, 2009, **311**, 4558–4569.
3 D. B. Trushina, T. V. Bukreeva and M. N. Antipina, *Cryst. Growth Des.*, 2016, **16**, 1311–1319.
4 S. C. Huang, K. Naka and Y. Chujo, *Langmuir*, 2007, **23**, 12086–12095.
5 X. R. Xu, A. H. Cai, R. Liu, H. H. Pan, R. K. Tang and K. Cho, *J. Cryst. Growth*, 2008, **310**, 3779–3787.
6 D. Konopacka-Łyskawa, *Crystals*, 2019, **9**, 223.
7 Y. Boyjoo, V. K. Pareek and J. Liu, *J. Mater. Chem. A*, 2014, **2**, 14270–14288.
8 P. Fadia, S. Tyagi, S. Bhagat, A. Nair, P. Panchal, H. Dave, S. Dang and S. Singh, *3 Biotech*, 2021, **11**, 1–30.
9 A. Vikulina, J. Webster, D. Voronin, E. Ivanov, R. Fakhrullin, V. Vinokurov and D. Volodkin, *Mater. Des.*, 2021, **197**, 109220.
10 M. Abebe, N. Hedin and Z. Z. Bacsik, *Cryst. Growth Des.*, 2015, **15**, 3609–3616.
11 H. Imai, N. Tochimoto, Y. Nishino, Y. Takezawa and Y. Oaki, *Cryst. Growth Des.*, 2012, **12**, 876–882.
12 C. Wang, C. He, Z. Tong, X. Liu, B. Ren and F. Zeng, *Int. J. Pharm.*, 2006, **308**, 160–167.
13 M. Lei, W. H. Tang, L. Z. Cao, P. G. Li and J. G. Yu, *J. Cryst. Growth*, 2006, **294**, 358–366.
14 Y. Wang, Y. X. Moo, C. Chen, P. Gunawan and R. Xu, *J. Colloid Interface Sci.*, 2010, **352**, 393–400.
15 A. Jada and A. Verraes, *Colloids Surf., A*, 2003, **219**, 7–15.
16 H. Kawaguchi, H. Hirai, K. Sakai, S. Seral, T. Nakajima, Y. Ebisawa and K. Koyama, *Colloid Polym. Sci.*, 1992, **270**, 1176–1181.
17 S. Ouhenia, D. Chateigner, M. A. Belkhir, E. Guilmeau and C. Krauss, *J. Cryst. Growth*, 2008, **310**, 2832–2841.

18 J. Yu, M. Lei, B. Cheng and X. Zhao, *J. Solid State Chem.*, 2004, **177**, 681–689.
19 J. Tark Han, X. Xu and K. Cho, *J. Cryst. Growth*, 2007, **308**, 110–116.
20 B. Cheng, M. Lei, J. Yu and X. Zhao, *Mater. Lett.*, 2004, **58**, 1565–1570.
21 H. Matahwa, V. Ramiah and R. D. Sanderson, *J. Cryst. Growth*, 2008, **310**, 4561–4569.
22 K. Naka, S. C. Huang and Y. Chujo, *Langmuir*, 2006, **22**, 7760–7767.
23 A. T. Nagaraja, S. Pradhan and M. J. McShane, *J. Colloid Interface Sci.*, 2014, **418**, 366–372.
24 I. M. Weiss, N. Tuross, L. Addadi, S. Weiner, E. Beniash and J. Aizenberg, *Proc. R. Soc. London, Ser. B*, 2001, **135**, 1875–1879.
25 H. Cölfen and L. Qi, *Chem.–Eur. J.*, 2001, **7**, 106–116.
26 S. Guragain, N. L. Torad, Y. G. Alghamdi, A. A. Alshehri, J. Kim, B. P. Bastakoti and Y. Yamauchi, *Mater. Lett.*, 2018, **230**, 143–147.
27 M. Lei, W. H. Tang and J. G. Yu, *Mater. Res. Bull.*, 2005, **40**, 656–664.
28 Ç. M. Oral and B. Ercan, *Powder Technol.*, 2018, **339**, 781–788.
29 G. Yan, L. Wang and J. Huang, *Powder Technol.*, 2009, **192**, 58–64.
30 L. Wang, Z. Meng, Y. Yu, Q. Meng and D. Chen, *Polymer*, 2008, **49**, 1199–1210.
31 Y. Tanaka and K. Naka, *Polym. J.*, 2010, **42**, 676–683.
32 Y. Tanaka and K. Naka, *Polym. J.*, 2012, **44**, 586–593.
33 R. Febrida, A. Cahyanto, E. Herda, V. Muthukanan, N. Djustiana, F. Faizal, C. Panatarani and I. M. Joni, *Materials*, 2021, **14**, 4425.
34 B. Cheng, J. Yu, T. Arisawa, K. Hayashi, J. J. Richardson, Y. Shibuta and H. Ejima, *Nat. Commun.*, 2022, **13**, 1892.
35 J. Yu, B. Cheng and H. Ejima, *J. Mater. Chem. B*, 2020, **8**, 6798–6801.
36 A. Wulf, R. I. Mendgaziev, R. Fakhrullin, V. Vinokurov, D. Volodkin and A. S. Vikulina, *Adv. Funct. Mater.*, 2022, **32**, 2109824.
37 F. Tewes, O. L. Gobbo, C. Ehrhardt and A. M. Healy, *ACS Appl. Mater. Interfaces*, 2016, **8**, 1164–1175.
38 X. H. Guo, S. H. Yu and G. B. Cai, *Angew. Chem., Int. Ed.*, 2006, **45**, 3977–3981.
39 X. Geng, L. Liu, J. Jiang and S. H. Yu, *Cryst. Growth Des.*, 2010, **10**, 3448–3453.
40 M. S. Rao, *Bull. Chem. Soc. Jpn.*, 1973, **46**, 1414–1417.
41 D. V. Volodkin, A. I. Petrov, M. Prevot and G. B. Sukhorukov, *Langmuir*, 2004, **20**, 3398–3406.
42 C. B. Tovani, D. C. Zancanela, A. N. Faria, P. Ciancaglini and A. P. Ramos, *J. Mater. Chem.*, 2011, **6**, 90509–90515.
43 A. G. Christy, *Cryst. Growth Des.*, 2017, **17**, 3567–3578.
44 L. N. Zhao, J. K. Wang and Z. C. Wang, *Chem. Res. Chin. Univ.*, 2013, **29**, 969–973.